

## MATERIAL MODEL OF THE $\text{AlCu}_2\text{SiMn}$ ALLOY UNDER HOT PLASTIC FORMING <sup>(1)</sup>

A. G O N T A R Z and Z. P A T E R

METAL FORMING DEPARTMENT  
FACULTY OF MECHANICAL ENGINEERING  
TECHNICAL UNIVERSITY OF LUBLIN,  
ul. Nadbystrzycka 36, 20-618 Lublin, Poland

### NOTATIONS

$\alpha$	angle of shear strain,
$\gamma$	shear strain,
$\dot{\gamma}$	shear strain rate,
$\gamma_m$	shear strain at the external sample's layer,
$\varphi$	equivalent strain,
$\varphi_g$	limit strain,
$\dot{\varphi}$	equivalent strain rate,
$\theta$	angle of twist,
$\sigma_p$	flow stress,
$\tau$	shear stress in the cross-section of the sample,
$\omega$	twist rate,
$m$	strain rate sensitivity coefficient,
$n$	degree of the polynomial,
$p$	strain hardening coefficient,
$r$	distance from the sample axis,
$t$	temperature,
$A_1, A_2, \dots, A_n$	polynomial coefficients,
$B_1, B_2, \dots, B_n$	polynomial coefficients,
$C$	constant,
$L$	length of measurement part of the sample,
$M_s$	torque,
$N$	number of sample's rotations,
$R$	external radius of twisted sample

---

<sup>1)</sup> Paper presented at the 2nd Seminar "Integrated Study on the Foundations of Plastic Deformation of Metals", at Dąbrówka (near Łańcut, Poland) Nov. 16-19, 1998.

## 1. INTRODUCTION

The designing of metal forming processes is based on the knowledge of material's behaviour under deformation. The flow stress values are the most important parameters subject to change during forming. The modelling of forming processes is dependent on the flow stress values as functions of strain, strain rate and temperature. The functions describing those relationships are usually presented on plane diagrams called flow curves. They are obtained in experiments by using one of many known methods. Three basic ones are: tension, compression and torsion. The first one is rarely applied because of a limited range of available strains. The others are widely applied. Each of them has its own advantages and disadvantages and they need to be considered when a certain method is chosen. A large number of factors like available strain value, range of possible strain rates, way and costs of sample preparing, possibility of using digital equipment for controlling and measuring, availability of appropriate plastometers, kind of process to be modelled, need to be taken into account. This paper presents the results of the AlCu2SiMn aluminium alloy under the torsion test at the temperature range of 350 – 500 °C. The purpose was to create a material model of the AlCu2SiMn alloy and to determine the temperature range for hot forming of this alloy for modelling and experimental tests of cross-wedge rolling process.

## 2. DESCRIPTION OF TESTS

The test samples were made of AlCu2SiMn alloy extruded rod in forms and dimensions shown in Fig. 1.

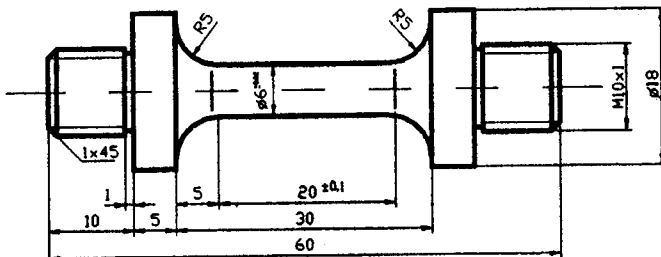


FIG. 1. Shape and dimensions of the tested specimen.

The torsion tests were carried out at a twist rate of 8.3 rpm, 750 rpm and 1500 rpm, which is equivalent to the strain rate values (according to Tresca hypothesis) of  $0.065 \text{ s}^{-1}$ ,  $5.9 \text{ s}^{-1}$ , and  $11.8 \text{ s}^{-1}$ . The tests were performed at the temperature range between 350 °C and 500 °C, because that is typical for hot plastic forming

of aluminium alloys. In order to compare the results with the compression tests, an additional test was performed at 18 °C.

### 3. INTERPRETATION OF THE TORSION TEST

The flow curve is determined in most cases under the assumption that the twisted sample shows a non-uniform strain distribution across the sections and that the strain value is proportional to the distance from the sample axis. This may be illustrated by the following formula:

$$(3.1) \quad \operatorname{tg} \alpha = \gamma = \frac{r\theta}{L} = \frac{2\pi r N}{L}.$$

The non-uniform distribution of the strain in cross-section of a sample is caused by the inhomogeneity of the material hardening. The distribution of shear stress is usually described by the following formula:

$$(3.2) \quad \tau = C\gamma^p\gamma^m.$$

Provided that the sample sections remain plane during torsion and the sample length remains unchanged, the elementary torque  $dM_s$  acting on the layer at  $r$  radius and  $dr$  thickness is equal

$$(3.3) \quad dM_s = 2\pi r \cdot dr \cdot \tau(r) \cdot r.$$

Therefore, after integration and transformation, the following relationship describing the stress value in external sample layer is obtained:

$$(3.4) \quad \tau_m = \frac{M_s}{2\pi R^3} \cdot (3 + p + m).$$

The relationship (3.4) enables the calculation of the shear stress at the external layer of a full sample for a known torque  $M_s$  and known  $p$  and  $m$  values. In most cases, the  $p$  value is calculated as

$$(3.5) \quad p = \frac{\partial \ln M}{\partial \ln N}$$

at constant twist rate  $\omega$  and temperature  $t$ . The  $m$  value is equal to

$$(3.6) \quad m = \frac{\partial \ln M}{\partial \ln \omega}$$

at constant number of rotations  $N$  and temperature  $t$ .

The flow stress is calculated by using the Tresca hypothesis:

$$(3.7) \quad \sigma_p = 2\tau_m$$

or the Huber-Mises-Hencky's hypothesis:

$$(3.8) \quad \sigma_p = \sqrt{3} \cdot \tau_m.$$

The number of formulas used for calculating effective strains is much greater. Some of them are shown in Table 1.

**Table 1. Equations used to calculate the equivalent strain.**

No.	Author	The equation	No. of Eq.	References
1	Mises	$\varphi = \frac{\gamma_m}{\sqrt{3}}$	(3.9)	[1, 2, 3]
2	Tresca	$\varphi = \frac{\gamma_m}{2}$	(3.10)	[1, 2, 3]
3	Nadai-Mises	$\varphi = \frac{2}{\sqrt{3}} \ln \left( \frac{\gamma_m}{2} + \sqrt{\frac{\gamma_m^2}{4} + 1} \right) = \frac{2}{\sqrt{3}} \operatorname{arcsin} h \frac{\gamma_m}{2}$	(3.11)	[1, 2, 4, 5]
4	Nadai-Tresca	$\varphi = \ln \left( \frac{\gamma_m}{2} + \sqrt{\frac{\gamma_m^2}{4} + 1} \right) = \operatorname{arcsin} h \frac{\gamma_m}{2}$	(3.12)	[1, 2]
5	Hajduk-Mises	$\varphi = \ln \left( 1 + \frac{\gamma_m}{\sqrt{3}} \right)$	(3.13)	[1, 2]
6	Hajduk-Tresca	$\varphi = \ln \left( 1 + \frac{\gamma_m}{2} \right)$	(3.14)	[1, 2]
7	Morozumi	$\varphi = 2 \ln \sqrt{1 + \frac{2}{3} \gamma_m}$	(3.15)	[1, 2]
$\gamma_m = \frac{2\pi RN}{L}$			(3.16)	

The above table shows that the results of the torsion test may be interpreted in many various ways. It is difficult to evaluate the accuracy of the presented formulas and this is the reason for problems in choosing one of them for practical use. In order to select the proper formula, the authors have compared the flow curves obtained from the torsion test with the one obtained from the compression test.

To determine the distribution of shear stress over the twisted sample's cross-section, a special calculating method, using the  $n$ -degree polynomial for describing the shear stress was used:

$$(3.17) \quad \tau = A_0 + A_1 \cdot \gamma + A_2 \cdot \gamma^2 + \dots + A_n \cdot \gamma^n.$$

After using the relationships (3.1), (3.3) and (3.17), the formula expressing the torque  $M_s$  at the sample's section looks as follows:

$$(3.18) \quad M_s = 2\pi \int_0^R \left[ A_0 + A_1 \frac{2\pi Nr}{L} + A_2 \left( \frac{2\pi Nr}{L} \right)^2 + \dots + A_n \left( \frac{2\pi Nr}{L} \right)^n \right] \cdot r^2 dr,$$

and after integration, the final relationship describing the torque  $M_s$  is:

$$(3.19) \quad M_s = B_0 + B_1 \cdot N + B_2 \cdot N^2 + \dots + B_n \cdot N^n,$$

where:

$$(3.20) \quad B_0 = 2\pi A_0 \cdot \frac{R^3}{3}, \quad B_1 = 2\pi A_1 \cdot \frac{2\pi}{L} \cdot \frac{R^4}{4}, \\ B_2 = 2\pi A_2 \cdot \left( \frac{2\pi}{L} \right)^2 \cdot \frac{R^5}{5}, \dots, B_n = 2\pi A_n \cdot \left( \frac{2\pi}{L} \right)^n \cdot \frac{R^{n+3}}{n+3}.$$

The next stage is, to find such values of  $B_0, B_1, B_2 \dots B_n$ , which assure the minimal error between moment values obtained experimentally and calculated theoretically. To achieve it, the least squares approximation method may be used. Knowing the values of  $B_0, B_1, B_2 \dots B_n$  coefficients, the values of  $A_0, A_1, A_2 \dots A_n$  may be calculated and substituted to the Eq. (3.17) in order to determine the values of shear stress in the external layer of the sample ( $R = r$ ) at a known number of rotations  $N$ .

The flow curves at the torsion test were obtained by using the above described method as well as equations shown in Table 1. The results are shown in Fig. 2 together with the flow curve obtained from the compression test (at the same deformation conditions). This comparison showed that the compression curve is placed above all torsion curves. The family of curves obtained by applying the Tresca hypothesis for calculation of the stress is located closer to the "compression curve" than the "Mises curves". This result confirms the opinion expressed in the paper [3], that the Tresca hypothesis should be applied for non-iron metals and alloys.

Among some "Tresca curves", the curve for which the equivalent strain was calculated using the Hajduk-Tresca formula is located most closely to the "compression curve". However, the shape of that curve is different from the compression curve. For smaller strain values ( $\varphi < 0.6$ ), the stress calculated from the Hajduk-Tresca formula is lower than those obtained under compression. The remaining three "Tresca curves" are more similar to the "compression curve" (they

are more similar to the “compression curve” than the “Hajduk-Tresca curve”). This is the reason why the Tresca hypothesis was chosen for calculating both the flow stress and the equivalent strain.

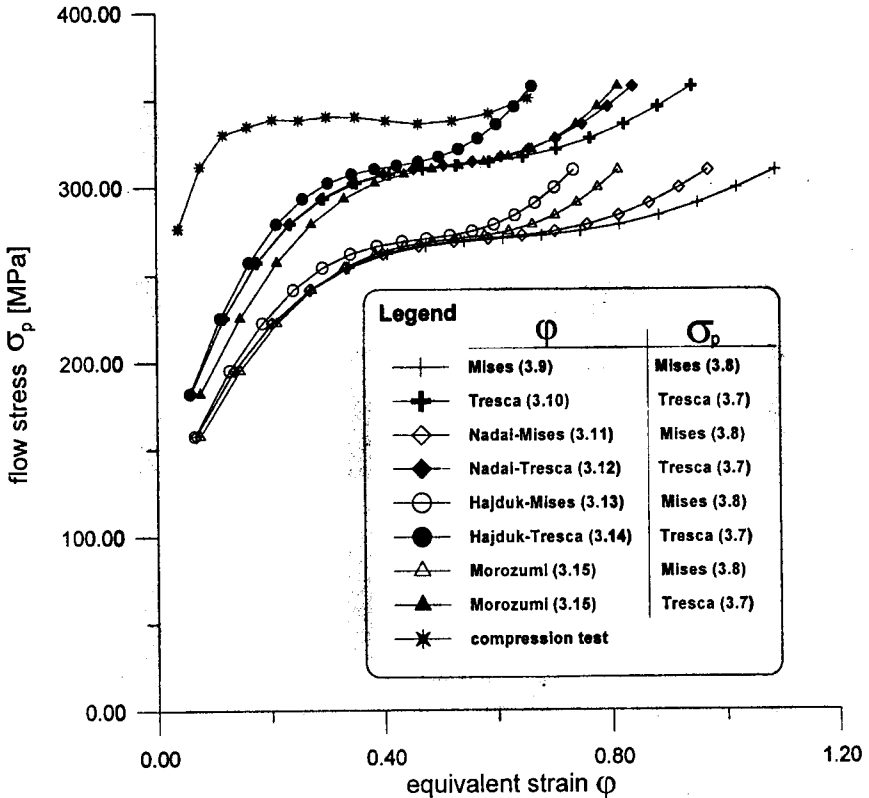


FIG. 2. Comparison between the flow curves obtained from compression and torsion tests.

#### 4. ANALYSIS OF THE TEST RESULTS

Figures 3, 4 and 5 show the flow curves for the AlCu2SiMn alloys at three different strain rates at temperature range of 350 °C – 500 °C.

The course of AlCu2SiMn alloy flow curves is characteristic for the whole range of temperatures and strain rates. At the first stage of deformation, the flow stress grows to its maximal value and then decreases. The magnitude of the stress increase and decrease changes depending on temperature and the strain rate. After a certain strain value corresponding to flow stress maximum is exceeded, it begins to decrease. This is the consequence of the dynamic recovery process occurring in the material.

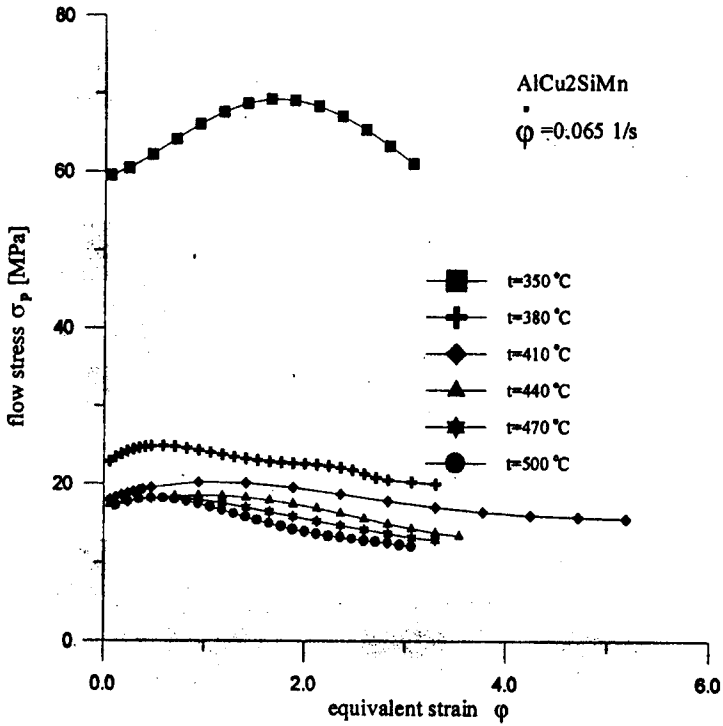


FIG. 3. Flow curves of AlCu<sub>2</sub>SiMn aluminium alloy obtained for strain rate 0.065 1/s.

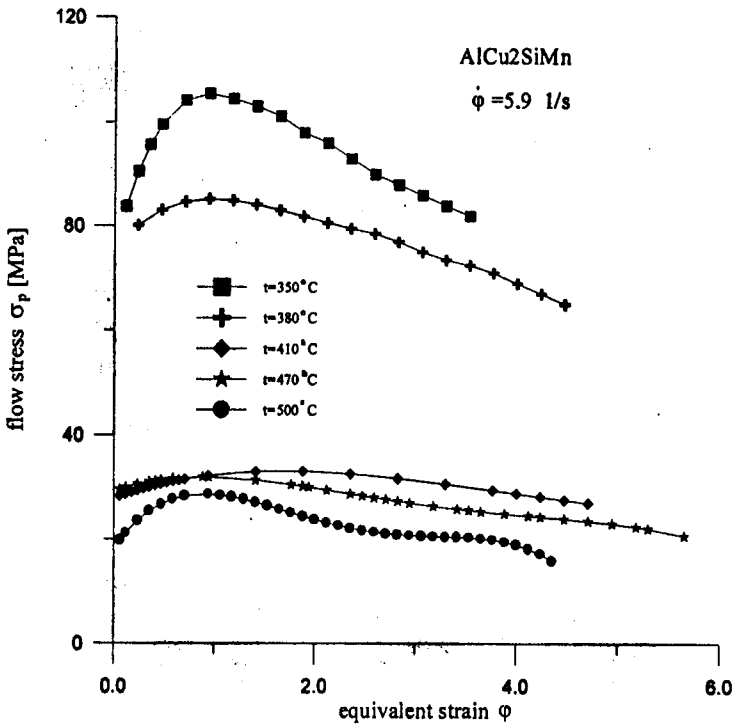


FIG. 4. Flow curves of AlCu<sub>2</sub>SiMn aluminium alloy obtained for strain rate 5.9 1/s.

The diagrams show a strong influence of temperature on the flow stress values. At each tested strain rate, there is a temperature range enabling a 2–3 times decrease of flow stress when the temperature rises by 30 °C. This proves that for a given strain rate, a specific limit temperature exists; after exceeding it, the restoration processes are strongly activated. This limit temperature determines the final hot working temperature and is respectively equal to 380 °C, 410 °C and 410 °C for strain rate values of 0.065 s<sup>-1</sup>, 5.9 s<sup>-1</sup>, and 11.8 s<sup>-1</sup>.

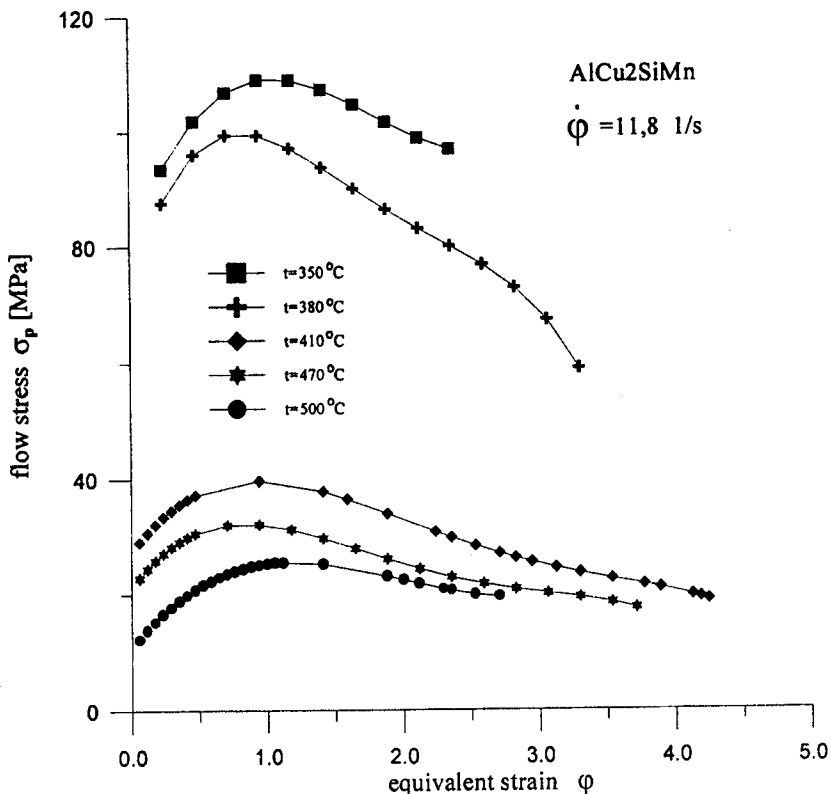


FIG. 5. Flow curves of AlCu<sub>2</sub>SiMn aluminium alloy obtained for strain rate 11.8 1/s.

The course of the curves at temperatures below the final forging limit temperatures is also characteristic. A strong drop of curves after reaching the maximum value can be noticed. Such the course is especially visible at the highest strain rate 11.8 s<sup>-1</sup> and temperature of 380 °C (Fig. 5). Within the temperature range between 380 °C and 410 °C, the decrease of flow stress value reaches even almost 50%. For that reason, even a small temperature growth above 380 °C caused by a thermal effect makes a rapid drop of the curve. This effect is more visible at higher strain rates because of a stronger temperature growth.

In order to determine the start hot-working temperature, the samples were deformed at 470 °C and 500 °C and afterwards subjected to structural testing. No overheating was found in both cases and it allowed to assume the 500 °C as the initial forging temperature.

Figure 6 shows the function of limit strains within the tested temperature range. The run of curves is similar for all strain rates. The limit strain value grows at lower temperatures up to its maximal value and then decreases at higher temperatures. Such a course is the evidence of existence of an optimal temperature in relation to the material's plastic properties. The existence of maximal plasticity at certain temperatures and at a constant strain rate is also described in other papers. In the paper [6] the authors (referring also to several other works concerning the plasticity of aluminium alloys) explain that a good plasticity at higher temperatures is a result of the dynamic recovery, which reduces the internal stresses. The level of dynamic recovery grows together with the temperature and increases the plasticity, but at certain temperatures diffusion processes occur and produce the vacancies. This causes the decrease of plasticity at higher temperatures than the one corresponding to the maximal limit strain value.

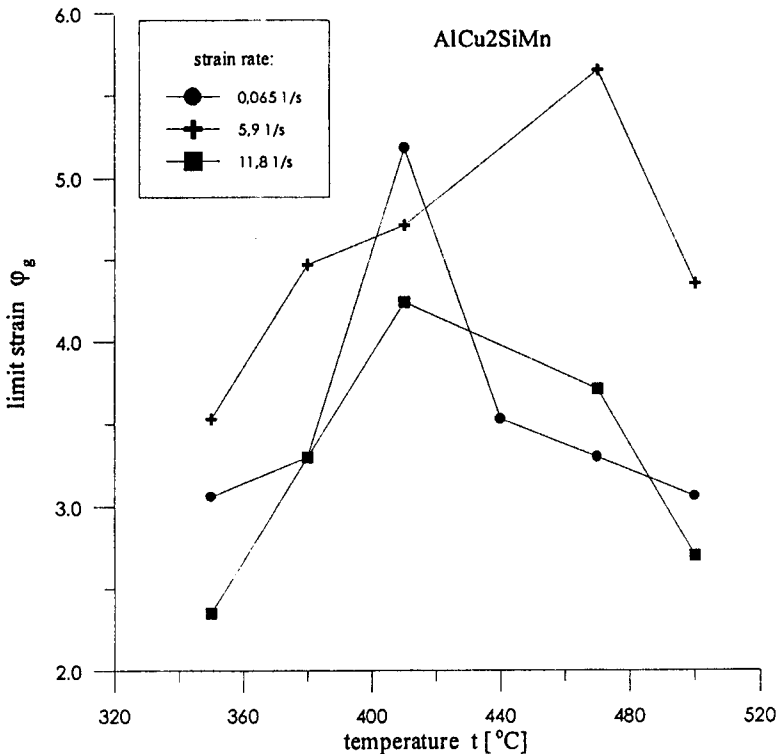


FIG. 6. Limit strains at the tested temperature range.

It must be emphasised that a temperature drop below the final hot working temperature results in a rapid increase of the flow stress. Therefore a special attention should be paid to maintaining the material temperature above the final hot working temperature. Pre-heating of dies is necessary in order to avoid a fast workpiece cooling.

The hot working start and final temperatures show that low strain rates are more convenient. The range of forming temperatures is wider than that at higher rates. The lower strain rates are better also for a weaker material hardening which reduces the power consumption and reduces the unit pressures exerted on the material-tool contact surface and this makes the tools more durable.

## 5. SUMMARY

The results of the torsion tests investigation of AlCu2MnSi aluminium alloy are presented in this paper. The experiments were carried out at the temperature range between 350 °C and 500 °C and at a twist rate of 8.3 rpm, 750 rpm and 1500 rpm. Various ways of interpretation of the torsion test were shown. A comparison between the results of torsion and compression tests was done, as well. Using the results of this comparison, the Tresca hypothesis was chosen for the calculation of both the flow stress and of the equivalent strain. The flow curves and the limit strain curves were obtained for investigated conditions. Moreover, the range of hot forming temperatures of the analysed alloy was estimated.

The obtained results were used for constructing the material model of AlCu2SiMn alloy. This model was used for the numerical simulation of the cross-wedge rolling process [7].

## ACKNOWLEDGEMENTS

The present study has been completed under the grant KBN No. 7 T08B 038 10 "Analysis of rolling process including upsetting by means of wedge tool segments".

## REFERENCES

1. T. SPITTEL, M. SPITTEL and J. SUCHANEK, *Untersuchung der thermischen Verhältnisse im Wärmtorsionsversuch*, Neue Hütte, **31**, 6, 233-238, 1986.
2. T. SPITTEL, M. SPITTEL and H. TEICHERT, *Umformeingenschaften von Aluminium und Aluminiumlegierungen*, Aluminium, **70**, 1/2, 68-76, 1994.

3. A.M. GAŁKIN, *Plastometer tests of metals and alloys*, Ed. Technical University of Częstochowa, Częstochowa 1990.
4. E. HADASIK, A. PLOCH, I. SCHINDLER and B. MACHULEC, *Utilization of computer techniques for plastometer research*, Proc. III Conference KomPlasTech'96, 8-10 January 1996 Koninki, 41-47.
5. I. SAUNDERS, J. NUTTING, *Deformation of metals to high strains using combination of torsion and compression*, Metal Science, **18**, 571-575, 1984.
6. A. FORCELESE, F. GABRIELLI, F. MICARI and O. ZURLA, *Computer simulation of metal flow in the hot upsetting of a high-strength aluminium alloy*, Journal of Materials Processing Technology, **39**, 83-99, 1993.
7. W. WEROŃSKI, A. GONTARZ and Z. PATER, *Forecasting of possible cross-wedge rolling of the AlCu<sub>2</sub>SiMn alloy*, Conference Proceedings 2 International Conference on Industrial Tools, Maribor-Rogaska Slatina, Slovenia, 1-5, 1999.

Received January 18, 1999.

---